SIAM J. SCI. COMPUT.
Vol. 40, No. 3, pp. A1362–A1385

COMBINING THE AUGMENTED LAGRANGIAN PRECONDITIONER WITH THE SIMPLE SCHUR COMPLEMENT APPROXIMATION*

XIN HE†, CORNELIS VUIK‡, AND CHRISTIAAN M. KLAIJ§

Abstract. The augmented Lagrangian (AL) preconditioner and its variants have been successfully applied to solve saddle point systems arising from the incompressible Navier–Stokes equations discretized by the finite element method. Attractive features are the purely algebraic construction and robustness with respect to the Reynolds number and mesh refinement. In this paper, we reconsider the application of the AL preconditioner in the context of the stabilized finite volume methods and present the extension to the Reynolds-averaged Navier–Stokes (RANS) equations, which are used to model turbulent flows in industrial applications. Furthermore, we propose a new variant of the AL preconditioner, obtained by substituting the approximation of the Schur complement from the SIMPLE preconditioner into the inverse of the Schur complement for the AL preconditioner. This new variant is applied to both Navier–Stokes and RANS equations to compute laminar and turbulent boundary-layer flows on grids with large aspect ratios. Spectral analysis shows that the new variant yields a more clustered spectrum of eigenvalues away from zero, which explains why it outperforms the existing variants in terms of the number of Krylov subspace iterations.

Key words. Reynolds–averaged Navier–Stokes equations, finite volume method, block structured preconditioner, augmented Lagrangian preconditioner, SIMPLE preconditioner

AMS subject classifications. 65F10, 65F08

DOI. 10.1137/17M1144775

1. Introduction.

The augmented Lagrangian (AL) preconditioner [2], belonging to the class of block structured preconditioners [9, 26, 27], is originally proposed to solve saddle point systems arising from the incompressible Navier–Stokes equations discretized by the finite element method (FEM). The AL preconditioner features a purely algebraic construction and robustness with respect to the Reynolds number and mesh refinement. Because of these attractive features, recent research was devoted to the further development and extension of the AL preconditioner, notably the modified variants [3, 4, 5] with reduced computational complexity and the extension [32] to the context of stabilized finite volume methods (FVM), which are widely used in industrial computational fluid dynamic (CFD) applications.

Although applying FEM and FVM to the incompressible Navier–Stokes equations both lead to saddle point systems, the extension from FEM to FVM is nontrivial; see [32] for a detailed discussion on the dimensionless parameter that is involved in the AL preconditioner, its influence on the convergence of both nonlinear and linear iterations, and the proposed rule to choose the optimal value in practice. We observed that the features of the AL preconditioner exhibited in the FEM context, e.g., robust-

*Submitted to the journal's Methods and Algorithms for Scientific Computing section August 24, 2017; accepted for publication (in revised form) February 20, 2018; published electronically May 10, 2018.

http://www.siam.org/journals/sisc/40-3/M114477.html

†State Key Laboratory of Computer Architecture, Institute of Computing Technology, Chinese Academy of Sciences, Zhongguancun Haidian District, Beijing, People's Republic of China 100190 (hexin2016@ict.ac.cn, http://english.ict.cas.cn/).

‡Delft Institute of Applied Mathematics, Delft University of Technology, Mekelweg 4, 2628 CD Delft, The Netherlands (c.vuik@tudelft.nl, http://www.ewi.tudelft.nl/).

§Maritime Research Institute Netherlands, 6700 AA Wageningen, The Netherlands (c.klaij@marin.nl, http://www.marin.nl/).

ness with respect to the Reynolds number and mesh refinement, are maintained in the context of FVM, at least for academic benchmarks. This motivates us to consider the application of the AL preconditioner in the broader context of Reynolds-averaged Navier–Stokes (RANS) equations, which are used to model turbulent flows in industrial CFD applications. These equations are obtained by applying the Reynolds averaging process to the Navier–Stokes equations and adding an eddy-viscosity turbulence model to close the system; see [11, 23, 30]. Such models represent the effect of turbulence on the averaged flow quantities through a locally increased viscosity.

Unfortunately, straightforward application of the AL preconditioner to the RANS equations yields disappointing results, as we will show in this paper. Therefore, we reconsider the approximation of the Schur complement, which is the key to the efficient block structured preconditioners [1, 24]. In [15], we compared the exact Schur preconditioner with several cheaper approximations, including SIMPLE, for three test cases from maritime engineering, characterized by the thin turbulent boundary layers on grids with high aspect ratios. In this paper, we propose a new Schur complement approximation which leads to a new variant of the AL preconditioner. The approach is to substitute the approximation of the Schur complement from the SIMPLE preconditioner [14, 16] into the inverse of the Schur complement for the AL preconditioner. This choice is motivated by the notion that in the utilized FVM the Schur complement approximation from the SIMPLE preconditioner reduces to a scaled Laplacian matrix [14, 16] and the efficiency of the SIMPLE preconditioner on the complicated maritime applications [15, 16]. As we will show, the new variant of the AL preconditioner significantly speeds up the convergence rate of the Krylov subspace solvers for both turbulent and laminar boundary-layer flows computed with a stabilized FVM.

The structure of this paper is as follows. The RANS equations and the discretization and solution methods are introduced in section 2. The new method to construct the approximation of the Schur complement in the AL preconditioner is presented in section 3, followed by a brief recall of the old approach. A comparison with the SIMPLE preconditioner in section 3.4 is based on a basic cost model presented in section 4. Section 5 includes the numerical experiments carried out on the turbulent and laminar benchmarks. Conclusions and future work are outlined in section 6.

2. Governing equations and solution techniques. In this section, we introduce the Reynolds-averaged Navier–Stokes equations as well as the finite volume discretization and solution methods.

2.1. Reynolds-averaged Navier–Stokes equations. Incompressible and turbulent flows often occur in CFD applications of the maritime industry. Most commercial and open-source CFD packages rely on the Reynolds-averaged Navier–Stokes (RANS) equations to model such flows [11, 23, 30] since more advanced models, such as the large-eddy simulation (LES), are still too expensive for industrial applications. In addition, engineers are first interested in the averaged properties of a flow, such as the average forces on a body, which is exactly what RANS models provide.

The RANS equations are obtained from the Navier–Stokes equations by an averaging process referred to as Reynolds averaging, where an instantaneous quantity such as the velocity is decomposed into its averaged and fluctuating parts. If the flow is statistically steady, time averaging is used and ensemble averaging is applied for unsteady flows. The averaged part is solved, while the fluctuating part is modeled, which requires additional equations, for instance, for the turbulent kinetic energy and turbulence dissipation. We refer the reader to [11, 23, 30] for a broader discussion. The Reynolds-averaged equations are here presented in the conservative form using

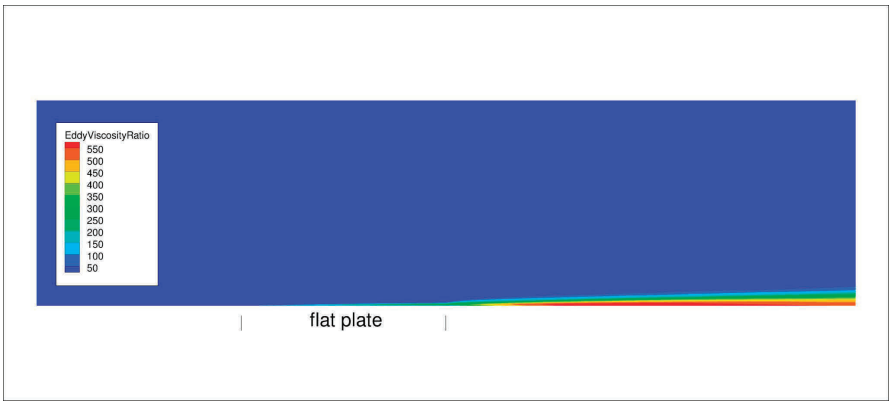

FIG. 1. *For the turbulent flat plate problem, the ratio between the eddy viscosity and dynamic viscosity, i.e., μ_t/μ in the wake of the plate.*

FVM for a control volume Ω with the surface S and outward normal vector $\mathbf{n}$:

$$\int_S \rho \mathbf{u}\mathbf{u}\cdot\mathbf{n}\,dS + \int_S P\mathbf{n}\,dS - \int_S \mu_{\text{eff}}(\nabla\mathbf{u} + \nabla\mathbf{u}^T)\cdot\mathbf{n}\,dS = \int_\Omega \rho\mathbf{b}\,d\Omega, \tag{1}$$
$$\int_S \mathbf{u}\cdot\mathbf{n}\,dS = 0,$$

where $\mathbf{u}$ is the velocity, $P = p + \frac{2}{3}\rho k$ consists of the pressure p and the turbulent kinetic energy k, ρ is the (constant) density, μ_{eff} is the (variable) effective viscosity, and $\mathbf{b}$ is a given force field. On the boundaries we either impose the velocity ($\mathbf{u} = \mathbf{u}_{\text{ref}}$ on inflow and $\mathbf{u} = 0$ on walls) or the normal stress ($\mu_{\text{eff}}\frac{\partial\mathbf{u}}{\partial\mathbf{n}} - P\mathbf{n} = 0$ on outflow and far field). The effective viscosity μ_{eff} is the sum of the constant dynamic viscosity μ and the variable turbulent eddy viscosity μ_{t} provided by the turbulence model as a function of k and possibly other turbulence quantities. Notice that for laminar flows, where k and μ_{t} are zero, the RANS equations reduce to the Navier–Stokes equations.

In this paper, we will consider laminar flow of water over a finite flat plate at $\text{Re} = 10^5$ and turbulent flow at $\text{Re} = 10^7$. The density and dynamic viscosity of water at atmospheric pressure and 20 degrees Celsius are roughly $\rho = 1000[\text{kg/m}^3]$ and $\mu = 0.001[\text{kg/m/s}]$; see [31]. The inflow velocity $\mathbf{u}_{\text{ref}}$ in [m/s] is adjusted to obtain the given Reynolds number $\text{Re} = \frac{\rho\|\mathbf{u}_{\text{ref}}\|L_{\text{ref}}}{\mu}$ based on the length $L_{\text{ref}} = 1[\text{m}]$ of the plate. The flow is characterized by a very thin boundary layer on the plate which is fully resolved by stretching the grid in the vertical direction. This inevitably results in high aspect-ratio cells near the plate. At the higher Reynolds number, the flow becomes turbulent in this thin boundary layer and in the wake of the plate. Figure 1 illustrates how the effective viscosity (provided in this case by the k-ω shear stress transport model of Menter [20]) varies in the domain: the eddy viscosity in the wake of the plate is two orders of magnitude larger than the dynamic viscosity. We also consider turbulent flow over a backward-facing step at Reynolds $5 \cdot 10^4$ based on the step height, which has a similar eddy-viscosity magnitude in the wake of the step.

Solvers for the RANS equations should be able to handle both challenges, i.e., the high-aspect ratio cells and the significant variation in viscosity.

2.2. Linear saddle point system. As explained in [15], the nonlinear system (1) is solved for $\mathbf{u}$ and P as a series of linear systems obtained by the Picard linearization [11], i.e., by assuming that the mass flux $\rho\mathbf{u}\cdot\mathbf{n}$, the turbulent kinetic energy k,

and the effective viscosity μ_{eff} are known from the previous iteration. The turbulence equations are then solved for k and possibly other turbulence quantities, after which the process is repeated until a convergence criterion is met.

After linearization and discretization of system (1) by the cell-centered and collocated FVM [11], the linear system is in saddle point form as

$$\begin{bmatrix} Q & G \\ D & C \end{bmatrix} \begin{bmatrix} \mathbf{u} \\ p \end{bmatrix} = \begin{bmatrix} \mathbf{f} \\ g \end{bmatrix} \quad \text{with} \quad \mathcal{A} := \begin{bmatrix} Q & G \\ D & C \end{bmatrix}, \tag{2}$$

where Q corresponds to the convection-diffusion operator and the matrices G and D denote the gradient and divergence operators, respectively. The matrix C comes from the stabilization method. The details of these matrices are presented as follows.

The linearization and the explicit treatment of the second diffusion term $\mu_{\text{eff}} \nabla \mathbf{u}^T \cdot \mathbf{n}$ by using the velocity and effective viscosity from the previous iteration make the matrix Q of a block diagonal form. Each diagonal part Q_{ii} is equal and contains the contributions from the convective term $\rho u_i \mathbf{u} \cdot \mathbf{n}$ and the remaining diffusion term $\mu_{\text{eff}} \nabla u_i \cdot \mathbf{n}$.

In FEM the divergence matrix is the negative transpose of the gradient matrix, i.e., $D = -G^T$. However, in FVM we have $D_i = G_i$ on structured and unstructured grids, where i denotes the components therein. For structured grids only we have that D is skew-symmetric ($D_i = -D_i^T$) and therefore that $D = -G^T$ as in FEM. We refer the reader to [11] for the details of D and G in FVM.

To avoid pressure oscillations when the velocity and pressure are collocated in the cell centers, the pressure-weighted interpolation (PWI) method [21] is applied here and leads to the stabilization matrix C as

$$C = D\text{diag}^{-1}(Q)G - \text{diag}^{-1}(Q_{ii})L_p, \tag{3}$$

where L_p is the Laplacian matrix. Details about the PWI method and its representation by the discrete matrices as (3) are given in [14, 16].

2.3. Preconditioners for saddle point systems. Block structured preconditioners are used to accelerate the convergence rate of the Krylov subspace solvers for saddle point systems as (2). They are based on the block $\mathcal{LDU}$ decomposition of the coefficient matrix given by

$$\mathcal{A} = \mathcal{LDU} = \begin{bmatrix} Q & G \\ D & C \end{bmatrix} = \begin{bmatrix} I & O \\ DQ^{-1} & I \end{bmatrix} \begin{bmatrix} Q & O \\ O & S \end{bmatrix} \begin{bmatrix} I & Q^{-1}G \\ O & I \end{bmatrix}, \tag{4}$$

where $S = C - DQ^{-1}G$ is the so-called Schur complement. To successfully design block structured preconditioners, a combination of this block factorization with a suitable approximation of the Schur complement is utilized. It is not practical to explicitly form the exact Schur complement due to the action of Q^{-1} typically when the size is large. This implies that constructing the spectrally equivalent and numerically cheap approximations of the Schur complement can be very challenging. There exist several state-of-the-art approximations of the Schur complement, e.g., the least-squares commutator (LSC) [8], pressure convection-diffusion (PCD) operator [13, 28], SIMPLE(R) preconditioner [16, 17, 29], and augmented Lagrangian (AL) approach [2, 3, 4, 32]. These Schur complement approximations are originally designed in the context of stable FEM where the $(2, 2)$ block of $\mathcal{A}$ is zero. For more details of the Schur approximation, we refer the reader to the surveys [1, 24, 26, 27] and the books [9, 22].

This paper is meant to significantly improve the efficiency of the AL preconditioner in the turbulent and laminar boundary-layer flows computed with a stabilized FVM. To fulfill the objective of this paper, a new variant of the AL preconditioner is proposed which substitutes the approximation of the Schur complement from the SIMPLE preconditioner into the inverse of the Schur complement for the AL preconditioner. More details are presented in the next section.

3. Augmented Lagrangian preconditioner. In this section, we propose the new method to construct the approximation of the Schur complement in the AL preconditioner, followed by a comparison with the old approach.

3.1. Transformation of the linear system. It is observed in [2, 3] that applying the AL preconditioner allows us to circumvent the challenging issue of constructing the numerically cheap and spectrally equivalent approximation of the Schur complement S of the original system (2). To apply the AL preconditioner, the original system (2) is transformed into an equivalent one with the same solution [3, 32], which is of the form

$$\begin{bmatrix} Q_\gamma & G_\gamma \\ D & C \end{bmatrix} \begin{bmatrix} \mathbf{u} \\ p \end{bmatrix} = \begin{bmatrix} \mathbf{f}_\gamma \\ g \end{bmatrix} \quad \text{with} \quad \mathcal{A}_\gamma := \begin{bmatrix} Q_\gamma & G_\gamma \\ D & C \end{bmatrix}, \tag{5}$$

where $Q_\gamma = Q - \gamma G W^{-1} D$, $G_\gamma = G - \gamma G W^{-1} C$, and $\mathbf{f}_\gamma = \mathbf{f} - \gamma G W^{-1} g$. The scalar $\gamma > 0$ and the matrix W should be nonsingular. This transformation is obtained by multiplying $-\gamma G W^{-1}$ on both sides of the second row of system (2) and adding the resulting equation to the first one. Clearly, the transformed system (5) has the same solution as system (2) for any value of γ and any nonsingular matrix W. The Schur complement of $\mathcal{A}_\gamma$ is $S_\gamma = C - D Q_\gamma^{-1} G_\gamma$.

The equivalent system (5) is what we want to solve when applying the AL preconditioner. Using the block $\mathcal{DU}$ decomposition of $\mathcal{A}_\gamma$, the ideal AL preconditioner $\mathcal{P}_{\text{IAL}}$ is given by

$$\mathcal{P}_{\text{IAL}} = \begin{bmatrix} Q_\gamma & G_\gamma \\ O & \widetilde{S}_\gamma \end{bmatrix}, \tag{6}$$

where $\widetilde{S}_\gamma$ denotes the approximation of S_γ.

The modified variant of the ideal AL preconditioner, i.e., the so-called modified AL preconditioner, replaces Q_γ by its block lower-triangular part, i.e., $\widetilde{Q}_\gamma$, such that the difficulty of solving subsystems with Q_γ is avoided [3]. To see it more clearly, we take a 2D case as an example and give Q_γ and $\widetilde{Q}_\gamma$ as follows:

$$Q = \begin{bmatrix} Q_1 & O \\ O & Q_1 \end{bmatrix}, \; G = \begin{bmatrix} G_1 \\ G_2 \end{bmatrix}, \; D = \begin{bmatrix} D_1 & D_2 \end{bmatrix},$$

$$Q_\gamma = \begin{bmatrix} Q_1 - \gamma G_1 W^{-1} D_1 & -\gamma G_1 W^{-1} D_2 \\ -\gamma G_2 W^{-1} D_1 & Q_1 - \gamma G_2 W^{-1} D_2 \end{bmatrix},$$

$$\widetilde{Q}_\gamma = \begin{bmatrix} Q_1 - \gamma G_1 W^{-1} D_1 & O \\ -\gamma G_2 W^{-1} D_1 & Q_1 - \gamma G_2 W^{-1} D_2 \end{bmatrix}.$$

Substituting $\widetilde{Q}_\gamma$ into $\mathcal{P}_{\text{IAL}}$ as (6), we then get the modified AL preconditioner $\mathcal{P}_{\text{MAL}}$:

$$\mathcal{P}_{\text{MAL}} = \begin{bmatrix} \widetilde{Q}_\gamma & G_\gamma \\ O & \widetilde{S}_\gamma \end{bmatrix}. \tag{7}$$

It appears that one needs to solve subsystems with $\widetilde{Q}_\gamma$ when applying $\mathcal{P}_{\mathrm{MAL}}$. This work is further reduced to solve systems with $Q_1-\gamma G_1 W^{-1} D_1$ and $Q_1-\gamma G_2 W^{-1} D_2$. These two subblocks do not contain the coupling between two components of the velocity so that it is much easier to solve, compared to Q_γ involved in $\mathcal{P}_{\mathrm{IAL}}$.

3.2. New Schur complement approximation. The key of the ideal and modified AL preconditioners is to find a numerically cheap and spectrally equivalent Schur complement approximation $\widetilde{S}_\gamma$. The novel approximation proposed by this paper is based on the following lemma.

LEMMA 3.1. *Assuming that all the relevant matrices are invertible, then the inverse of S_γ is given by*

$$S_\gamma^{-1} = S^{-1}(I-\gamma C W^{-1}) + \gamma W^{-1}, \tag{8}$$

where $S = C - DQ^{-1}G$ denotes the Schur complement of the original system (2).

Proof. We refer the reader to [3, 32] for the proof. ∎

This lemma was already published, but its importance was not fully appreciated. Since Lemma 3.1 gives the connection between the Schur complement S_γ and S, it provides a framework to build the approximation of S_γ. Provided an approximation of S denoted by $\widetilde{S}$, it is natural to substitute $\widetilde{S}$ into expression (8) to construct an approximation of S_γ in the inverse form as

$$\widetilde{S}_{\gamma\ \mathrm{new}}^{-1} = \widetilde{S}^{-1}(I-\gamma C W^{-1}) + \gamma W^{-1}, \tag{9}$$

where the notation *new* is used to differ from the old approach to approximate S_γ, discussed in the next section.

Actually it is not necessary to explicitly implement $\widetilde{S}_{\gamma\ \mathrm{new}}$. Solving a subsystem with $\widetilde{S}_{\gamma\ \mathrm{new}}$, i.e., $\widetilde{S}_{\gamma\ \mathrm{new}}\ \mathbf{x} = \mathbf{b}$, converts to multiply the vector $\mathbf{b}$ on both sides of expression (9). Suppose that W is a diagonal matrix, e.g., the mass matrix M_p with density multiplied with cell volumes in FVM; then the complexity of $(\widetilde{S}^{-1}(I - \gamma C W^{-1}) + \gamma W^{-1})\mathbf{b}$ is focused on solving the system with $\widetilde{S}$. This means that the accelerating techniques to optimize $\widetilde{S}$ can reduce the computational time of the new approach.

From expression (9) it is clear that the Schur complement approximation $\widetilde{S}$ proposed for the original system (2) is used to construct $\widetilde{S}_{\gamma\ \mathrm{new}}$ here. Among the known LSC, PCD, and SIMPLE methods, this paper chooses the Schur complement approximation arising from the SIMPLE preconditioner. One motivation is that in the context of the considered FVM the Schur complement approximation from the SIMPLE preconditioner reduces to a scaled Laplacian matrix. See the next paragraph for more details. This choice is also motivated by the efficiency of the SIMPLE preconditioner on the complicated maritime applications; see [15, 16], for instance. We expect that the choice of the Schur complement approximation arising from the SIMPLE preconditioner helps to build a numerically cheap and efficient $\widetilde{S}_{\gamma\ \mathrm{new}}$.

Regarding the Schur complement $S = C - DQ^{-1}G$ of the original system (2), the SIMPLE preconditioner approximates Q by its diagonal, i.e., $\mathrm{diag}(Q)$, and obtains the approximation of S as $\widetilde{S}_1 = C - D\mathrm{diag}^{-1}(Q)G$. Taking into account the stabilization matrix $C = D\mathrm{diag}^{-1}(Q)G - \mathrm{diag}^{-1}(Q_{ii})L_p$ as given in (3), we further reduce the approximation to $\widetilde{S}_{\mathrm{SIMPLE}} = -\mathrm{diag}^{-1}(Q_{ii})L_p$ because the term $D\mathrm{diag}^{-1}(Q)G$ in $\widetilde{S}_1$ and C cancels. See, for instance, [14, 16] for a detailed discussion of obtaining $\widetilde{S}_{\mathrm{SIMPLE}}$

in FVM. Substituting $\widetilde{S}_{\text{SIMPLE}}$ and $W = M_p$ into expression (9), we obtain

$$\widetilde{S}_{\gamma\ \text{new}}^{-1} = \widetilde{S}_{\text{SIMPLE}}^{-1}(I - \gamma C M_p^{-1}) + \gamma M_p^{-1}, \text{ where } \widetilde{S}_{\text{SIMPLE}} = -\text{diag}^{-1}(Q_{ii})L_p. \tag{10}$$

Based on the above approach, it is easy to see that there is no extra requirement on the value of the parameter γ. As pointed out in the next section, the requirements in the old approximation of the Schur complement are contradictory. This suggests that the convergence rate of the Krylov subspace solvers preconditioned by the AL preconditioner with the new Schur complement approximation is weakly depending on the value of γ. This advantage makes the new AL variant less sensitive to the choice of γ. See the results regarding the influence of γ on the convergence rate in the numerical experiment section.

3.3. Old Schur complement approximation. For a comparison reason, the old approximation of the Schur complement in the AL preconditioner is recalled in this section. The starting point to construct the old approximation of the Schur complement in the AL preconditioner is also Lemma 3.1. However, the strategy is totally different. Choosing $W_1 = \gamma C + M_p$ and substituting W_1 into expression (8), we have

$$\begin{aligned} S_\gamma^{-1} &= S^{-1}(I - (\gamma C + M_p - M_p)(\gamma C + M_p)^{-1}) + \gamma(\gamma C + M_p)^{-1} \\ &= S^{-1}M_p(\gamma C + M_p)^{-1} + \gamma(\gamma C + M_p)^{-1} \\ &= (\gamma^{-1}S^{-1}M_p + I)(C + \gamma^{-1}M_p)^{-1}. \end{aligned}$$

For large values of γ such that $\| \gamma^{-1}S^{-1}M_p \| \ll 1$, the term $\gamma^{-1}S^{-1}M_p$ can be neglected so that we have $\widetilde{S}_{\gamma\ \text{old}}$ as follows:

$$\widetilde{S}_{\gamma\ \text{old}} = C + \gamma^{-1}M_p. \tag{11}$$

The choice of $W_1 = \gamma C + M_p$ is not practical since the action of W_1^{-1} is needed in the transformed system (5). The ideal and modified AL preconditioners, used, for instance, in [3, 32], omit the term γC in W_1 and choose $W = M_p$. The choice $W = M_p$ only involves the mass matrix M_p, which is easily inverted, especially in FVM, where M_p is a diagonal matrix.

The contradictory requirements in the above method are presented as follows. The approximation $\widetilde{S}_{\gamma\ \text{old}}$ is obtained if and only if $W_1 = \gamma C + M_p$ and large values of γ are chosen. However, $W = M_p$ is close to $W_1 = \gamma C + M_p$ only when γ is small. This means that it is contradictory to tune the value of γ so that $W = M_p$ and $\widetilde{S}_{\gamma\ \text{old}}$ could be simultaneously obtained. A simply balanced value of γ is $\gamma = 1$ or $O(1)$. This disadvantage reflects in the convergence rate of the Krylov subspace solvers. This paper shows that for the laminar calculations the number of the Krylov subspace iterations preconditioned by the AL preconditioner with $\widetilde{S}_{\gamma\ \text{old}}$ is about fourteen times larger than the new Schur approximation $\widetilde{S}_{\gamma\ \text{new}}$. An application of the AL preconditioner with $\widetilde{S}_{\gamma\ \text{old}}$ in the more challenging turbulent computations with variable viscosity and more stretched grids shows a very slow convergence or even stagnation. See numerical experiments in section 5.

In summary, regarding the ideal and modified AL preconditioners applied to the transformed system (5), there are two types of Schur complement approximations, i.e.,

1. $\widetilde{S}_{\gamma\ \text{new}}^{-1} = \widetilde{S}_{\text{SIMPLE}}^{-1}(I - \gamma C M_p^{-1}) + \gamma M_p^{-1}$, $\widetilde{S}_{\text{SIMPLE}} = -\text{diag}^{-1}(Q_{ii})L_p$,

2. $\widetilde{S}_{\gamma\ \mathrm{old}} = C + \gamma^{-1} M_p$.

The choice of $W = M_p$ is fixed in the transformation to obtain the equivalent system (5) and the construction of two Schur complement approximations.

3.4. SIMPLE preconditioner. Although the focus of this paper is on the new Schur complement approximation and its advantage over the old one in the AL preconditioner, we also present the SIMPLE preconditioner for a more comprehensive comparison. Different from the ideal AL preconditioner and its modified variant, the SIMPLE preconditioner is proposed for the original system (2), which is based on the block $\mathcal{LDU}$ decomposition of the coefficient matrix $\mathcal{A}$ and given by

$$\mathcal{P}_{\mathrm{SIMPLE}} = \begin{bmatrix} Q & O \\ D & \widetilde{S} \end{bmatrix} \begin{bmatrix} I & \mathrm{diag}^{-1}(Q)G \\ O & I \end{bmatrix},$$

where $\widetilde{S}$ denotes the approximation of the Schur complement of $\mathcal{A}$, i.e., $S = C - DQ^{-1}G$. With the stabilization matrix C given by (3), the Schur complement approximation becomes $\widetilde{S} = \widetilde{S}_{\mathrm{SIMPLE}} = -\mathrm{diag}^{-1}(Q_{ii})L_p$, where L_p is the Laplacian matrix. Therefore, the scaled Laplacian matrix is used as the approximation of the Schur complement in the SIMPLE preconditioner. In order to avoid repetition, we refer the reader to section 3.2 for the details of obtaining $\widetilde{S}_{\mathrm{SIMPLE}}$, and to [15, 16] for the performance of the SIMPLE preconditioner in the FVM context on both academic and maritime applications.

4. Cost model for AL and SIMPLE preconditioners. To summarize the linearized systems where the AL and SIMPLE preconditioners are applied individually, we give the schematic diagram as follows:

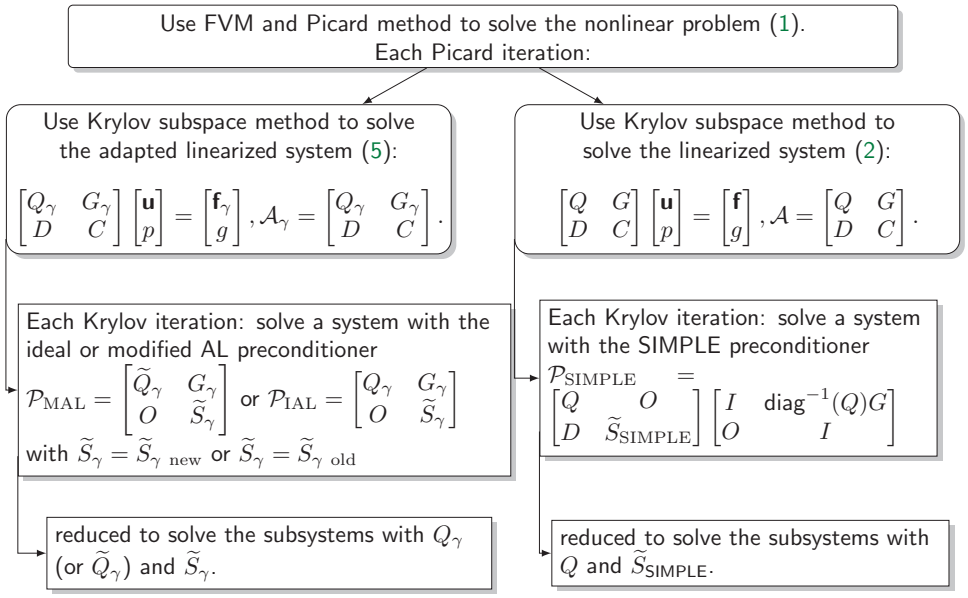

In [15], we presented a basic cost model to distinguish between the SIMPLE preconditioner and other preconditioners. Here, we extend the model to include the modified AL preconditioner with two Schur complement approximations. First, we consider the cost of using the SIMPLE preconditioner $\mathcal{P}_{\mathrm{SIMPLE}}$ for a Krylov subspace

method that solves the system with $\mathcal{A}$ to a certain relative tolerance in n_1 iterations. The preconditioner is applied at each Krylov iteration, and the SIMPLE preconditioner involves the solution of the momentum subsystem "mom-u" with Q and the pressure subsystem "mass-p" with $\widetilde{S}_{\text{SIMPLE}}$. In addition, at each Krylov iteration another cost is expressed in the product of the coefficient matrix $\mathcal{A}$ with a Krylov residual vector $\mathbf{b}_{res}$. Thus, the total cost is

- $\mathcal{P}_{\text{SIMPLE}}$: $n_1 \times$ (mom-u with Q + mass-p with $\widetilde{S}_{\text{SIMPLE}} + \mathcal{A} \times \mathbf{b}_{res}$).

Second, we consider the cost of applying the modified AL preconditioner $\mathcal{P}_{\text{MAL}}$ with the new Schur approximation $\widetilde{S}_{\gamma\ \text{new}}$. If we neglect the multiplications in the definition of $\widetilde{S}_{\gamma\ \text{new}}$ as given in (10), the cost of solving the pressure subsystem with $\widetilde{S}_{\gamma\ \text{new}}$ is the same as $\widetilde{S}_{\text{SIMPLE}}$. Thus, the total cost is

- $\mathcal{P}_{\text{MAL}}$ with $\widetilde{S}_{\gamma\ \text{new}}$: $n_2 \times$(mom-u with $\widetilde{Q}_\gamma$ +mass-p with $\widetilde{S}_{\text{SIMPLE}} + \mathcal{A}_\gamma \times \mathbf{b}_{res}$).

Finally, we consider the cost of applying the modified AL preconditioner $\mathcal{P}_{\text{MAL}}$ with the old Schur approximation $\widetilde{S}_{\gamma\ \text{old}}$. Similarly to the analysis of $\mathcal{P}_{\text{MAL}}$ with $\widetilde{S}_{\gamma\ \text{new}}$, we obtain the total cost as

- $\mathcal{P}_{\text{MAL}}$ with $\widetilde{S}_{\gamma\ \text{old}}$: $n_3 \times$ (mom-u with $\widetilde{Q}_\gamma$ + mass-p with $\widetilde{S}_{\gamma\ \text{old}} + \mathcal{A}_\gamma \times \mathbf{b}_{res}$).

Clearly, the difference in cost by applying $\mathcal{P}_{\text{MAL}}$ with $\widetilde{S}_{\gamma\ \text{new}}$ and $\widetilde{S}_{\gamma\ \text{old}}$ arises from solving the pressure subsystems with $\widetilde{S}_{\text{SIMPLE}}$ and $\widetilde{S}_{\gamma\ \text{old}}$, respectively. It is difficult to analytically compare the complexity of solving the subsystems with $\widetilde{S}_{\text{SIMPLE}}$ and $\widetilde{S}_{\gamma\ \text{old}}$. However, numerical experiments in the next section show $n_2 \ll n_3$ on all considered problems, which makes the new Schur complement approximation more efficient and attractive in terms of the number of iterations and wall-clock time.

At each Krylov iteration, more nonzero fill-in introduced in the blocks Q_γ and G_γ and more difficulty of iteratively solving the momentum subsystem with $\widetilde{Q}_\gamma$ than Q lead to a higher cost of applying $\mathcal{P}_{\text{MAL}}$ with $\widetilde{S}_{\gamma\ \text{new}}$ than $\mathcal{P}_{\text{SIMPLE}}$. We refer the reader to [32] for a detailed discussion. Therefore, this higher cost of $\mathcal{P}_{\text{MAL}}$ with $\widetilde{S}_{\gamma\ \text{new}}$ only pays off if $n_2 < n_1$. In this paper we observe $n_2 < n_1$ on the turbulent and laminar tests, but the time advantage of $\mathcal{P}_{\text{MAL}}$ with $\widetilde{S}_{\gamma\ \text{new}}$ over $\mathcal{P}_{\text{SIMPLE}}$ needs a further assessment, which is included in the future research plan.

5. Numerical experiments. In this section, we compare the new AL variant with the old one and the SIMPLE preconditioner, for incompressible and laminar flow governed by the Navier–Stokes equations, as well as turbulent flow governed by the Reynolds–averaged Navier–Stokes equations.

5.1. Flow over a finite flat plate (FP). Flow over a finite flat plate is a standard test case in maritime engineering; see [25] for a detailed study of various turbulence models with MARIN's CFD software package ReFRESCO [19].

We first consider the fully turbulent flow at $\text{Re} = 10^7$ on the block structured grids. The grids are refined near the leading and trailing edge of the plate and spread out in the wake of the plate; see Figure 2(a), which leads to some eccentricity and nonorthogonality. As can be seen, the grids are stretched in both the horizontal and vertical directions and reach the maximal aspect ratio of order $1 : 10^4$ near the middle of the plate. The complete flow is computed, starting from uniform laminar flow upstream of the plate.

Second, we reconsider laminar flow at $\text{Re} = 10^5$ on a straight single-block grid. This case was already presented in [14, 15, 16, 32] for other solvers and preconditioners. We reconsider it here to show that the new Schur complement approximation also improves the efficiency of the AL preconditioner in the calculations of laminar flow.

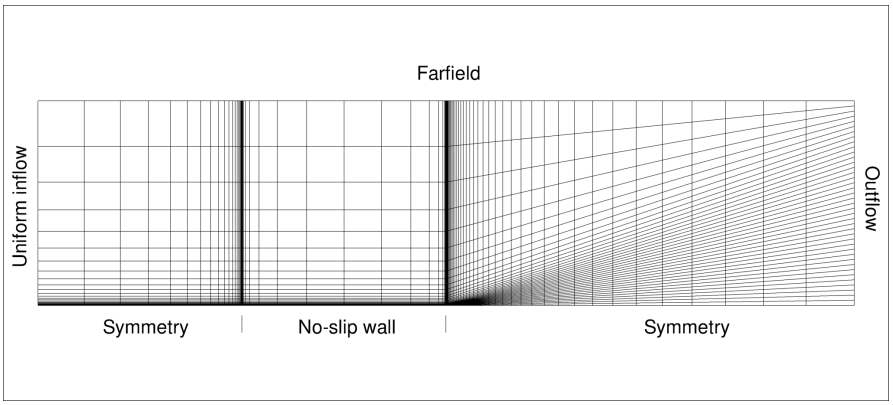

(a) Turbulent case

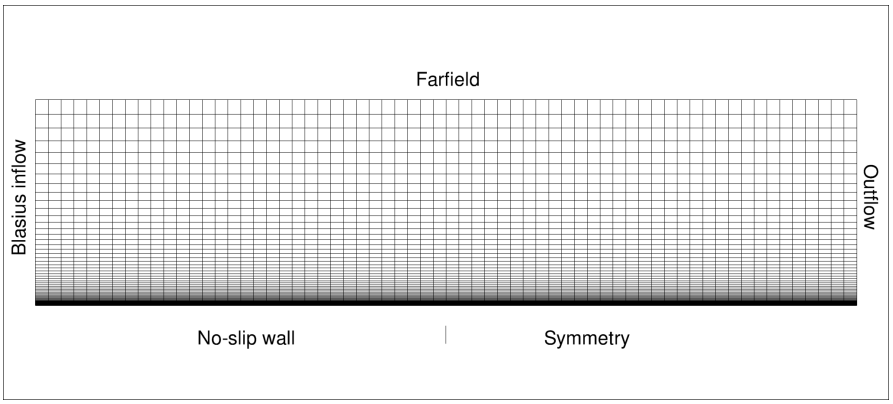

(b) Laminar case

FIG. 2. *Impression of the grids. Turbulent case with* 80×40 *cells and the max aspect ratio of order* $1:10^4$ *and laminar case with* 64×64 *cells and the max aspect ratio of order* $1:50$.

The stretched grids shown in Figure 2(b) are generated based on uniform Cartesian grids by applying the stretching function from [16] in the vertical direction. Near the plate the grids have a maximal aspect ratio of order $1:50$, which is about two orders smaller than the turbulent grids. Contrary to the turbulent case, the flow starts with the (semianalytical) Blasius solution halfway down the plate, so only the second half and the wake are computed.

5.2. Flow over a backward-facing step (BFS). We consider turbulent flow over a backward-facing step in a channel, as measured by Driver and Seegmiller [6]. The chosen case corresponds to the C-30 case from the ERCOFTAC Classic Collection [10], with Reynolds number $5 \cdot 10^4$ based on the inflow velocity and the step height. The flow is more complicated than the flat-plate flow as it features separation, a free shear-layer, and reattachment. Detailed results with ReFRESCO for various turbulence models are found in [7], including results for the k-ω SST turbulence model [20] used here. The grid is also more complicated: multiple blocks are used to wrap the boundary layer around the step; see Figure 3.

In this paper all experiments are carried out based on the blocks Q, G, D, C, M_p, and L_p and the right-hand side vector rhs, which are obtained at the 30th

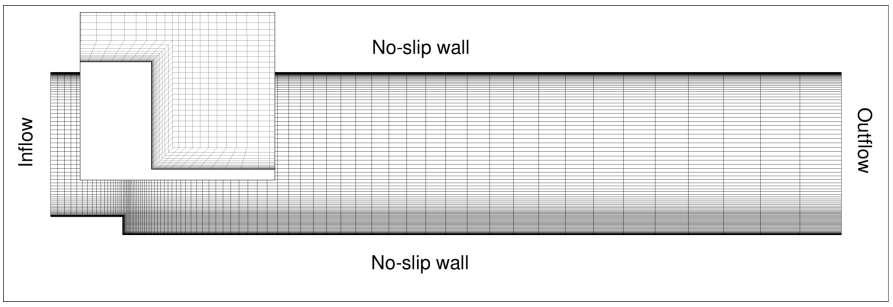

FIG. 3. *Impression of block structured grid with* 9600 *cells for turbulent flow over backward-facing step.*

nonlinear iteration. Numerical experiments in [32] show that the number of linear iterations varies during the nonlinear procedure. The motivation for choosing the 30th nonlinear iteration to export the blocks is that a representative number of linear iteration can be obtained from the 30th nonlinear step, compared with the average number of linear iterations through the whole nonlinear procedure. We use a series of structured grids with 80×40 and 160×80 cells for the turbulent FP case and the structured grid with 9600 cells for the turbulent BFS case. Regarding the laminar FP calculation, we use a structured grid with 64×64 cells. The matrices and right-hand side vector are generated by ReFRESCO and available in the MATLAB binary .mat format on the website [18]. The aim of the numerical experiments is to show the variation in the eigenvalues and the number of Krylov subspace iterations arising from different Schur complement approximations in the AL preconditioner. To carry out a comprehensive evaluation of the new Schur complement approximation in the AL preconditioner, in this paper we solve the linear system preconditioned by the AL preconditioner with the new Schur complement approximation to the machine accuracy. For a fair comparison, the same stopping tolerance is used when employing the old Schur complement approximation and the SIMPLE preconditioner. Since the AL preconditioner with different Schur complement approximations and the SIMPLE preconditioner involve various momentum or pressure subsystems, all the subsystems are directly solved in this paper to avoid the sensitiveness of iterative solvers on the varying solution complexities.

5.3. Numerical experiments on the turbulent FP case. To find out the reason that the new Schur complement approximation $\widetilde{S}_{\gamma\ \mathrm{new}}$ leads to a fast convergence of the Krylov subspace solvers preconditioned by the AL preconditioner, we plot ten extreme eigenvalues of the preconditioned matrices $\mathcal{P}_{\mathrm{IAL}}^{-1}\mathcal{A}_\gamma$ and $\mathcal{P}_{\mathrm{MAL}}^{-1}\mathcal{A}_\gamma$ with $\widetilde{S}_{\gamma\ \mathrm{new}}$ on the grid with 80×40 cells. The results, which are shown in Figures 4 and 5, show that for the considered values of γ the smallest eigenvalues are far from zero and the spectrum is clustered due to a small ratio between the largest and smallest magnitudes of the eigenvalues. Such a distribution of the eigenvalues is favorable for the Krylov subspace solvers and a fast convergence rate can be expected.

Results in Figure 6 show the fast convergence rate of the Krylov subspace solver preconditioned by the ideal AL preconditioner with the new Schur approximation $\widetilde{S}_{\gamma\ \mathrm{new}}$ on the grids with 80×40 cells and 160×80 cells. The fast convergence rate confirms the prediction that the new Schur approximation $\widetilde{S}_{\gamma\ \mathrm{new}}$ produces a favorable ideal AL preconditioner for the Krylov subspace solvers. In Figure 6 we observe that

large values of γ result in a faster convergence rate on both grids. This observation is analogous to that when applying the old Schur complement approximation $\widetilde{S}_{\gamma\ \mathrm{old}}$ in the ideal AL preconditioner with stable FEM; see [12], for instance. On the other hand, an ill-conditioned Q_γ can arise from large values of γ [32]. This indicates that the value of γ cannot be taken too large, otherwise solving the momentum subsystem with Q_γ can be very difficult. To circumvent the challenge of solving Q_γ with big values of γ and the slow convergence rate of the Krylov subspace solver by small values of γ, in this work we choose the balanced value of γ to be $\gamma = 1$ or $O(1)$ in the ideal AL preconditioner with the new Schur approximation $\widetilde{S}_{\gamma\ \mathrm{new}}$.

Compared with the ideal AL preconditioner, the values of γ exhibit a different influence on the spectrum of the preconditioned matrix by using the modified AL preconditioner. For example, with $\gamma = 100$ the smallest eigenvalue of $\mathcal{P}_{\mathrm{MAL}}^{-1}\mathcal{A}_\gamma$ is two orders of magnitude smaller than $\gamma = 0.01$ and $\gamma = 1.0$, as seen from the last row of Figure 5. It appears that the optimal value of γ, which leads to the most clustered eigenvalues of $\mathcal{P}_{\mathrm{MAL}}^{-1}\mathcal{A}_\gamma$, is $\gamma_{\mathrm{opt}} = 1$. Based on this observation we predict that the fastest convergence rate of the Krylov subspace solvers preconditioned by the modified AL preconditioner with $\widetilde{S}_{\gamma\ \mathrm{new}}$ can be obtained with $\gamma_{\mathrm{opt}} = 1$.

The convergence rates of the Krylov subspace solvers preconditioned by the modified AL preconditioner with $\widetilde{S}_{\gamma\ \mathrm{new}}$ on the grids with 80×40 cells and 160×80 cells are presented in Figure 7. We find out that $\gamma_{\mathrm{opt}} = 1$ results in the fastest convergence rate on two grids, and this confirms the prediction based on the spectrum analysis from Figure 5. Comparing two grids with 160×80 cells and 80×40 cells, it appears that the optimal value $\gamma_{\mathrm{opt}} = 1$ is independent of mesh refinement. This property is helpful in practice since one can carry out numerical experiments to determine γ_{opt} on coarse grids and then reuse it on finer grids.

In Table 1 we summarize the number of the Krylov subspace iterations preconditioned by the SIMPLE preconditioner and the AL preconditioners with the new Schur complement approximation $\widetilde{S}_{\gamma\ \mathrm{new}}$ and $\gamma = 1$ on two grids. First, we focus on the ideal and modified AL preconditioners. The value $\gamma = 1$ is a balanced choice for the ideal AL preconditioner and is the optimal choice for the modified AL preconditioner. As can be seen, for this considered turbulent case the new Schur complement approximation $\widetilde{S}_{\gamma\ \mathrm{new}}$ does not make the AL preconditioners independent of mesh refinement. This motivates a further study focused on mesh independence, which is planned as a future direction of research.

On the other hand, the proposal of the new Schur complement approximation $\widetilde{S}_{\gamma\ \mathrm{new}}$ is a big contribution to the development of AL preconditioners in the context of turbulent calculations. This is clearly seen from Figure 8, where the Krylov subspace solver converges very slowly when applying the old Schur complement approximation $\widetilde{S}_{\gamma\ \mathrm{old}}$ in the modified AL preconditioner. To understand this slow convergence the extreme eigenvalues of $\mathcal{P}_{\mathrm{MAL}}^{-1}\mathcal{A}_\gamma$ with $\widetilde{S}_{\gamma\ \mathrm{old}}$ on the grid with 80×40 cells are presented in Figure 9. We see that the smallest eigenvalues are quite close to zero for all tested values of γ, which degrades the efficiency of the Krylov subspace solver considerably. Among the tested values of γ, Figure 9 shows that $\gamma = 1$ results in a relatively clustered spectrum. Based on this observation we expect that the optimal value $\gamma_{\mathrm{opt}} = 1$ leads to the fastest convergence when using the old Schur complement approximation $\widetilde{S}_{\gamma\ \mathrm{old}}$ in the modified AL preconditioner. However, the number of Krylov subspace iterations preconditioned by $\mathcal{P}_{\mathrm{MAL}}$ with $\widetilde{S}_{\gamma\ \mathrm{old}}$ and $\gamma_{\mathrm{opt}} = 1$ is over 5000, as seen from Figure 8. Compared with 140 Krylov subspace iterations preconditioned by $\mathcal{P}_{\mathrm{MAL}}$ with $\widetilde{S}_{\gamma\ \mathrm{new}}$ and $\gamma_{\mathrm{opt}} = 1$, we clearly show that the new Schur complement

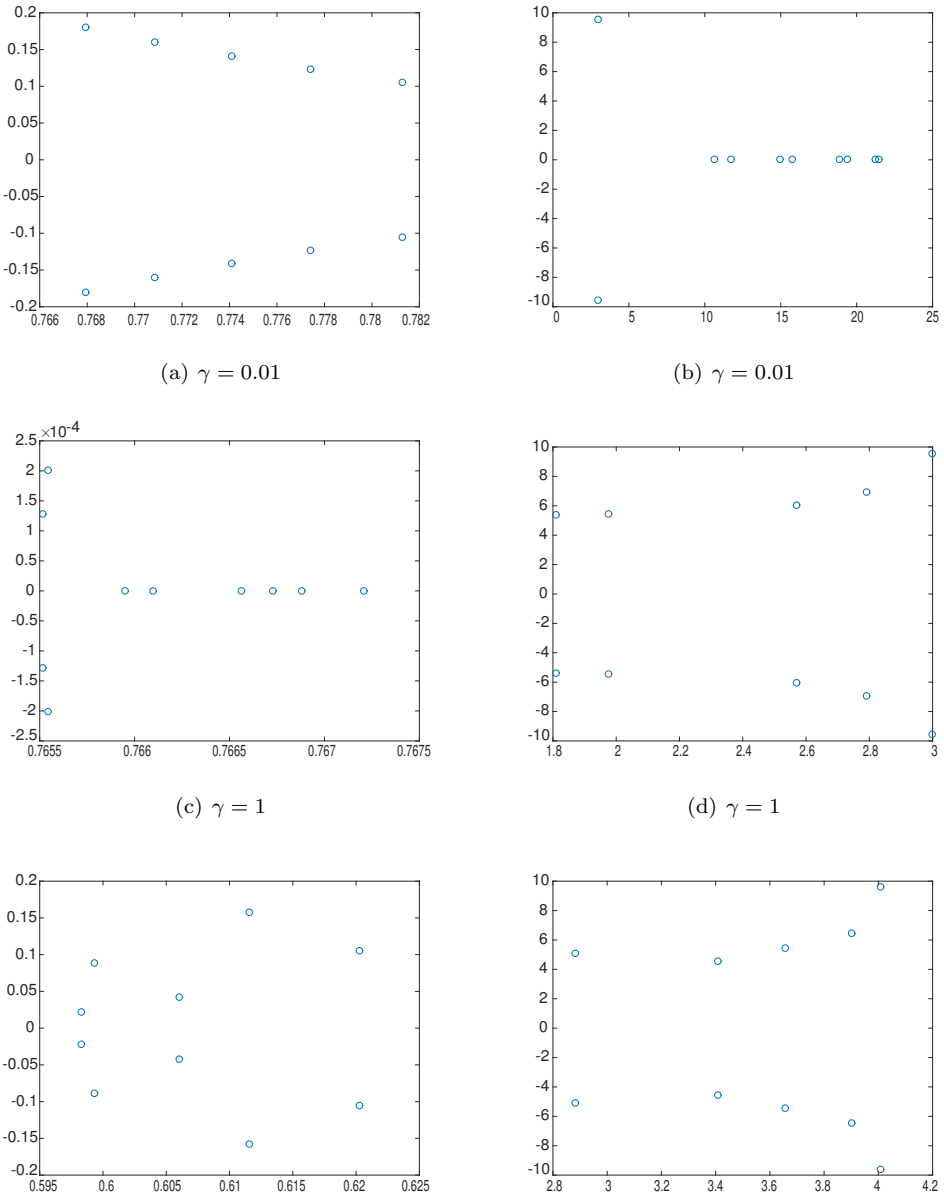

(a) $\gamma = 0.01$ (b) $\gamma = 0.01$

(c) $\gamma = 1$ (d) $\gamma = 1$

(e) $\gamma = 100$ (f) $\gamma = 100$

FIG. 4. *Turbulent FP: the ten smallest (left) and largest (right) eigenvalues of* $\mathcal{P}_{\text{IAL}}^{-1}\mathcal{A}_\gamma$ *with the new Schur approximation* $\widetilde{S}_{\gamma\ \text{new}}$ *and different values of* γ*. The grid with* 80×40 *cells is used.*

approximation $\widetilde{S}_{\gamma\ \text{new}}$ proposed in this paper significantly improves the performance of the AL preconditioners on the turbulent FP case.

Second, we compare the SIMPLE preconditioner with the modified AL preconditioner which uses the new Schur complement approximation $\widetilde{S}_{\gamma\ \text{new}}$ and $\gamma_{\text{opt}} = 1$. The

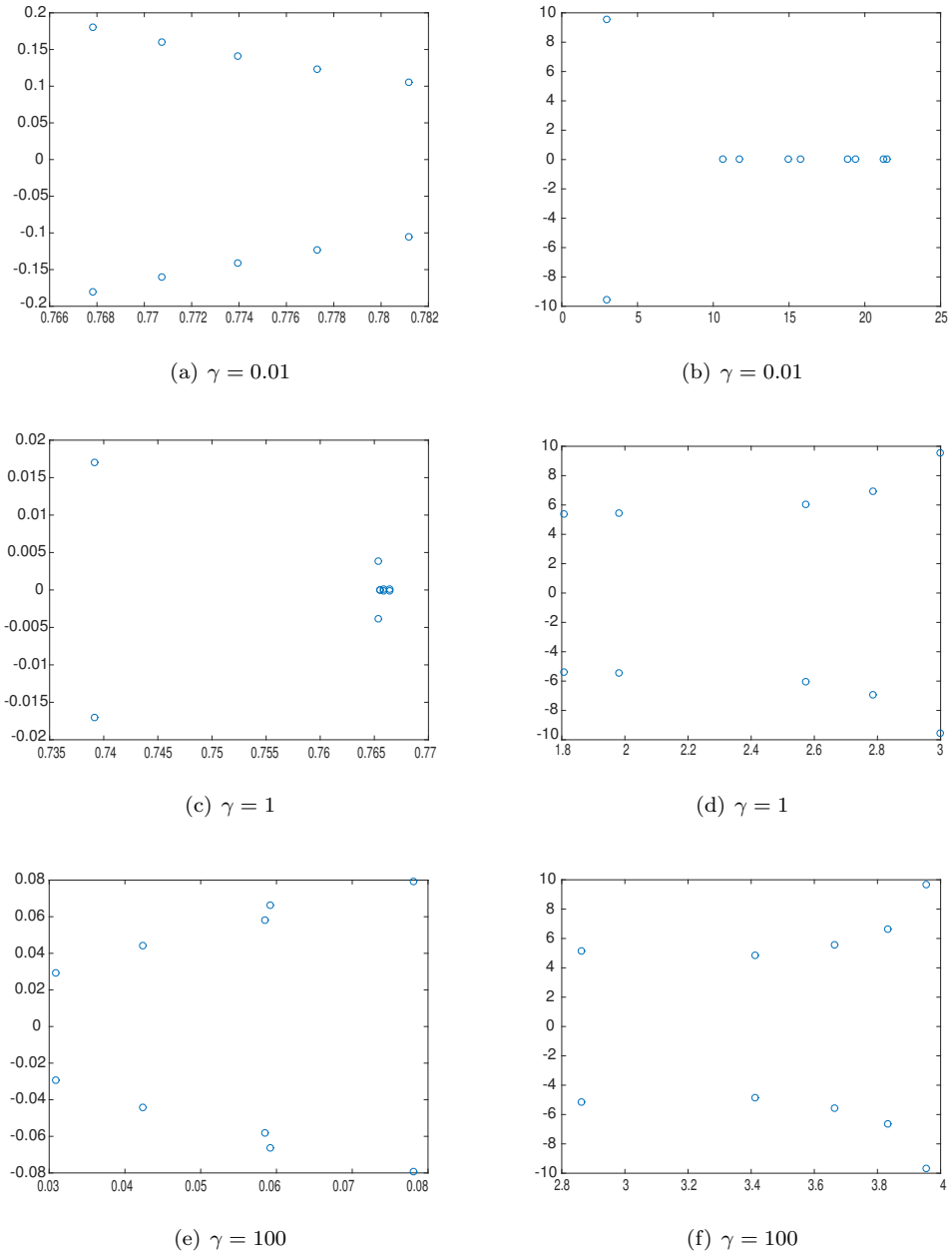

(a) $\gamma = 0.01$ (b) $\gamma = 0.01$

(c) $\gamma = 1$ (d) $\gamma = 1$

(e) $\gamma = 100$ (f) $\gamma = 100$

FIG. 5. *Turbulent FP: the ten smallest (left) and largest (right) eigenvalues of* $\mathcal{P}_{\mathrm{MAL}}^{-1}\mathcal{A}_\gamma$ *with the new Schur approximation* $\widetilde{S}_{\gamma\ \mathrm{new}}$ *and different values of* γ*. The grid with* 80×40 *cells is used.*

comparison in terms of the spectrum of the eigenvalues is given in Figure 10, which illustrates that on the grid with 80×40 cells the smallest eigenvalues are nearly the same for both preconditioners. However, the SIMPLE preconditioner leads to a larger ratio between the largest and smallest magnitudes of the eigenvalues, which means

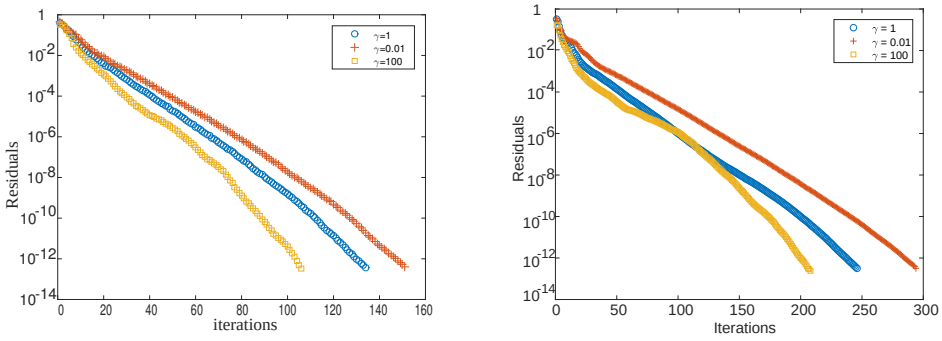

(a) Grid with 80×40 cells (b) Grid with 160×80 cells

FIG. 6. *Turbulent FP: the convergence of GMRES (no restart) preconditioned by the ideal AL preconditioner* $\mathcal{P}_{\text{IAL}}$ *with the new Schur approximation* $\widetilde{S}_{\gamma\ \text{new}}$ *on the grids with* 80×40 *cells (left) and* 160×80 *cells (right).*

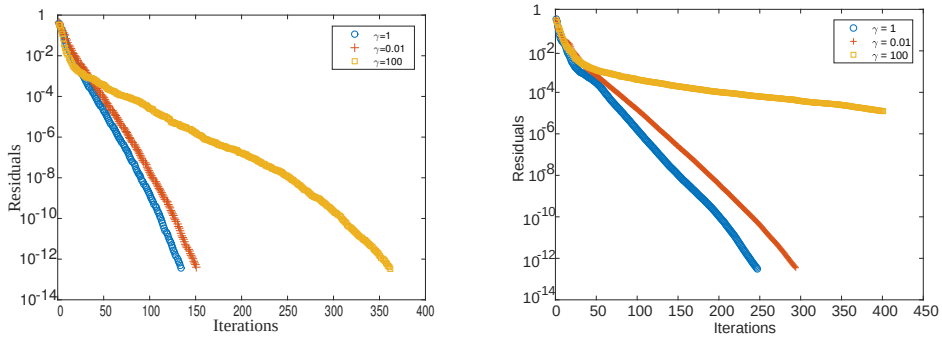

(a) Grid with 80×40 cells (b) Grid with 160×80 cells

FIG. 7. *Turbulent FP: the convergence of GMRES (no restart) preconditioned by the modified AL preconditioner* $\mathcal{P}_{\text{MAL}}$ *with the new Schur approximation* $\widetilde{S}_{\gamma\ \text{new}}$ *on the grids with* 80×40 *cells (left) and* 160×80 *cells (right).*

that the spectrum of the eigenvalues is less clustered compared to the modified AL preconditioner. Therefore, a faster convergence rate of the Krylov subspace solvers is expected by applying the modified AL preconditioner. Results in Table 1 illustrate that with the mesh refinement the number of Krylov subspace iterations increases by a factor of 1.7 by using the modified AL preconditioner with $\widetilde{S}_{\gamma\ \text{new}}$ and $\gamma_{\text{opt}} = 1$. The increasing factor is 2.2 when using the SIMPLE preconditioner. The smaller increasing factor allows a more apparent advantage of the modified AL preconditioner with $\widetilde{S}_{\gamma\ \text{new}}$ in terms of the reduced number of the Krylov subspace iterations with mesh refinement, which foresees the overall advantage in terms of total wall-clock time on fine enough grids.

5.4. Numerical experiments on the turbulent BFS case. On the calculations of the turbulent BFS case, we further assess the new Schur complement approximation $\widetilde{S}_{\gamma\ \text{new}}$ applied in the modified AL preconditioner and present the convergence

TABLE 1

Turbulent FP: the number of GMRES iterations (no restart) preconditioned by the SIMPLE preconditioner and the AL preconditioners with the new Schur approximation $\widetilde{S}_{\gamma\ \mathrm{new}}$ and $\gamma = 1$ on two grids.

Grid	80×40 cells	160×80 cells
$\mathcal{P}_{\mathrm{IAL}}$:	132	245
$\mathcal{P}_{\mathrm{MAL}}$:	140	246
$\mathcal{P}_{\mathrm{SIMPLE}}$:	180	382

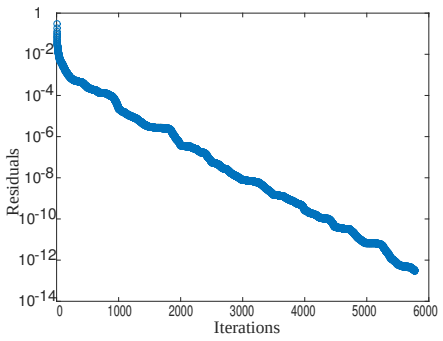

FIG. 8. *Turbulent FP: the convergence of GMRES (no restart) preconditioned by the modified AL preconditioner $\mathcal{P}_{\mathrm{MAL}}$ with the old Schur approximation $\widetilde{S}_{\gamma\ \mathrm{old}}$ and $\gamma_{opt} = 1$. The grid with 80×40 cells is used.*

rate of the Krylov subspace solver in Figure 11(a). As seen, the utilization of $\widetilde{S}_{\gamma\ \mathrm{new}}$ produces quite a fast convergence rate in the turbulent BFS case too. Among the considered values of γ, it appears that $\gamma_{\mathrm{opt}} = 0.1$ results in the fastest convergence rate on the turbulent BFS case. Considering $\gamma_{\mathrm{opt}} = 1$ on the turbulent FP test, we find out that the optimal value of γ resulting in the best performance of the modified AL preconditioner with the new Schur complement approximation $\widetilde{S}_{\gamma\ \mathrm{new}}$ is weakly problem dependent.

Comparable to the turbulent FP case, on the turbulent BFS test we also see the faster convergence rate achieved by using the modified AL preconditioner with $\widetilde{S}_{\gamma\ \mathrm{new}}$ than the SIMPLE preconditioner. Comparison in Figure 11(a) shows that the number of Krylov subspace iterations preconditioned by the modified AL preconditioner with $\widetilde{S}_{\gamma\ \mathrm{new}}$ and $\gamma_{\mathrm{opt}} = 0.1$ is nearly half that when using the SIMPLE preconditioner. Based on the result with mesh refinement in the turbulent FP case (see Table 1), it is reasonable to expect that in the turbulent BFS test fewer Krylov subspace iterations preconditioned by the modified AL preconditioner with $\widetilde{S}_{\gamma\ \mathrm{new}}$ will convert to a time advantage over the SIMPLE preconditioner on fine grids.

To illustrate the improvement arising from the utilization of the new Schur complement approximation $\widetilde{S}_{\gamma\ \mathrm{new}}$, in Figure 11(b) we present the convergence rate preconditioned by the modified AL preconditioner with the old Schur complement approximation $\widetilde{S}_{\gamma\ \mathrm{old}}$. The fastest convergence rate with $\widetilde{S}_{\gamma\ \mathrm{old}}$ is obtained with $\gamma_{\mathrm{opt}} = 1$, and other values of γ cannot make the solution procedure converge to the desired tolerance within the maximal 1000 iterations. The fastest convergence rate with $\widetilde{S}_{\gamma\ \mathrm{old}}$ and $\gamma_{\mathrm{opt}} = 1$ is about eight times slower than $\widetilde{S}_{\gamma\ \mathrm{new}}$ with $\gamma_{\mathrm{opt}} = 0.1$. The turbulent BFS case is another example to illustrate the advantage of the new Schur approximation $\widetilde{S}_{\gamma\ \mathrm{new}}$ over the old one $\widetilde{S}_{\gamma\ \mathrm{old}}$ in the turbulent context.

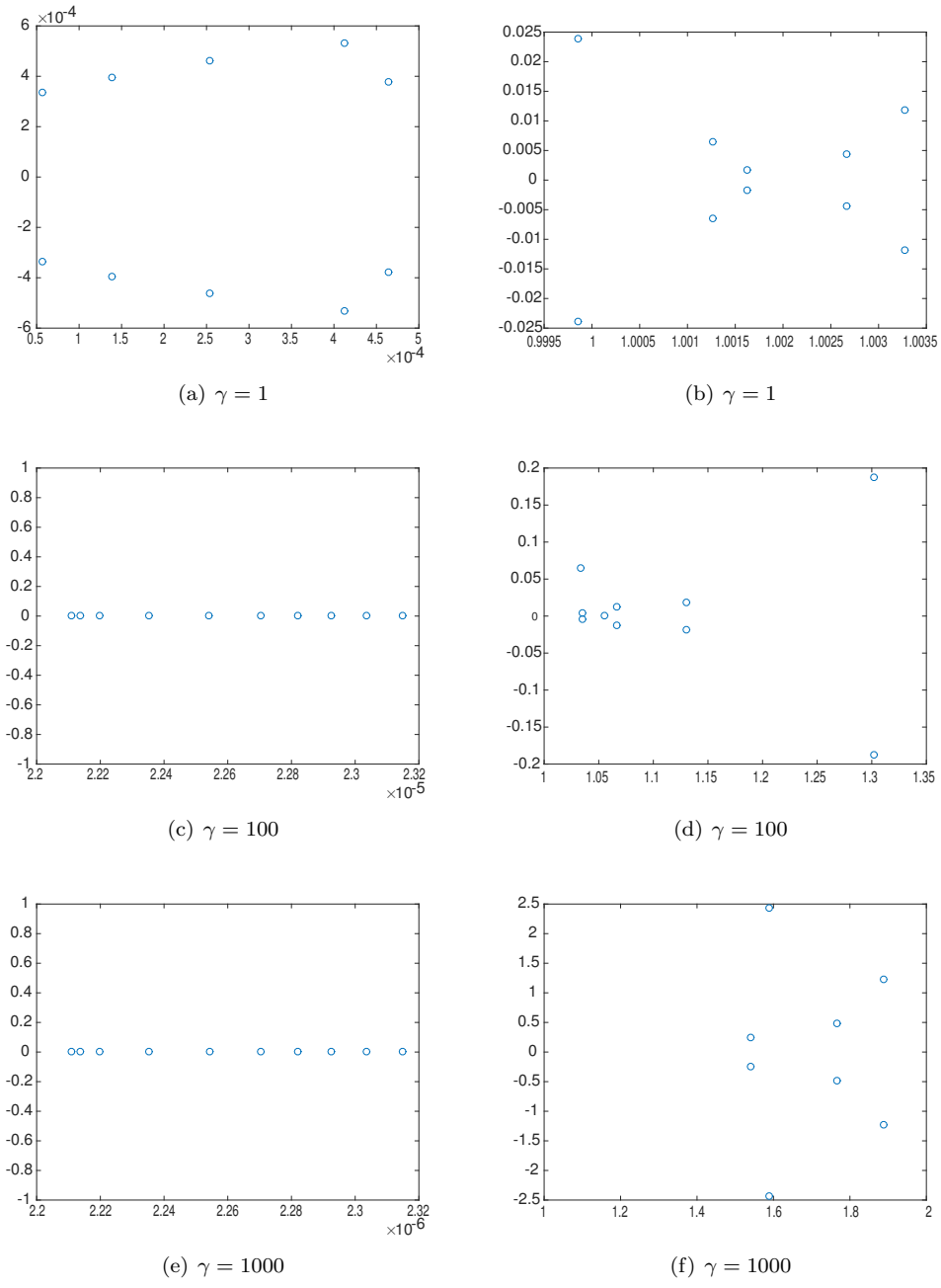

(a) $\gamma = 1$ (b) $\gamma = 1$

(c) $\gamma = 100$ (d) $\gamma = 100$

(e) $\gamma = 1000$ (f) $\gamma = 1000$

FIG. 9. *Turbulent FP: the ten smallest (left) and largest (right) eigenvalues of* $\mathcal{P}_{\mathrm{MAL}}^{-1}\mathcal{A}_\gamma$ *with the old Schur approximation* $\widetilde{S}_{\gamma\ \mathrm{old}}$ *and different values of* γ*. The grid with* 80×40 *cells is used.*

For a comprehensive comparison, in Table 2 we summarize the number of Krylov subspace iterations accelerated by different preconditioners. Since we have observed the mesh dependence of the AL preconditioners with the new Schur approximation $\widetilde{S}_{\gamma\ \mathrm{new}}$ on the turbulent FP case, we expect an analogous behavior in the turbulent

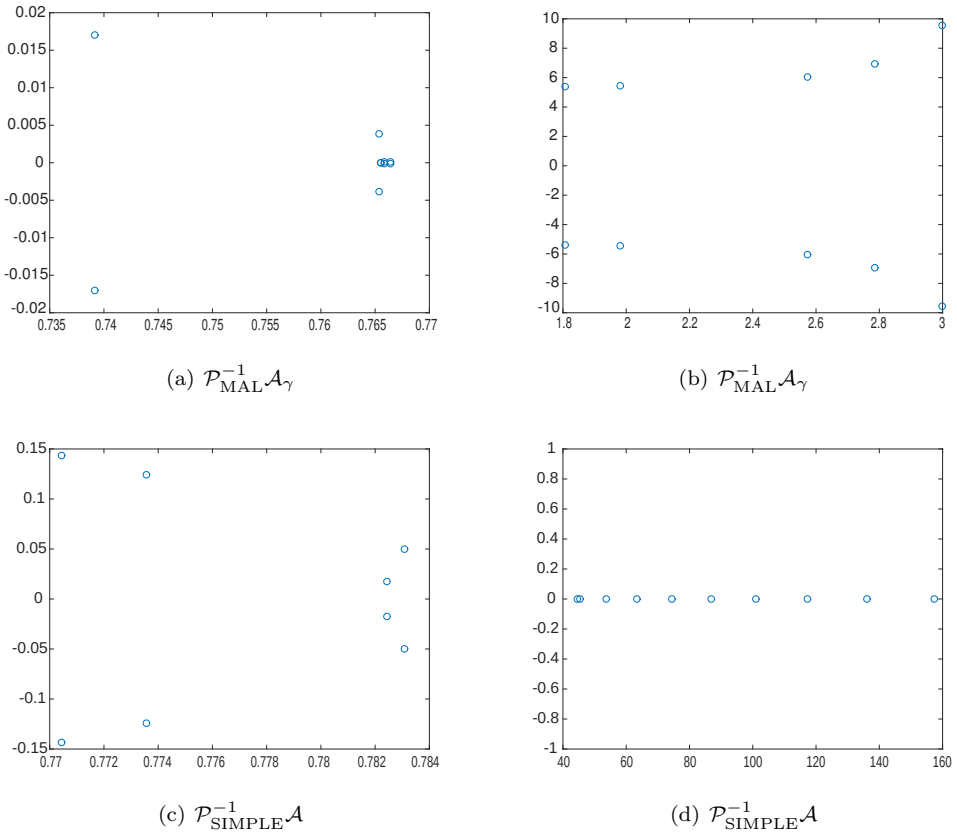

(a) $\mathcal{P}_{\mathrm{MAL}}^{-1}\mathcal{A}_\gamma$ (b) $\mathcal{P}_{\mathrm{MAL}}^{-1}\mathcal{A}_\gamma$

(c) $\mathcal{P}_{\mathrm{SIMPLE}}^{-1}\mathcal{A}$ (d) $\mathcal{P}_{\mathrm{SIMPLE}}^{-1}\mathcal{A}$

FIG. 10. *Turbulent FP: the ten smallest (left) and largest (right) eigenvalues of* $\mathcal{P}_{\mathrm{MAL}}^{-1}\mathcal{A}_\gamma$ *with the new Schur approximation* $\widetilde{S}_{\gamma\ \mathrm{new}}$ *and* $\gamma_{opt} = 1$*, and of* $\mathcal{P}_{\mathrm{SIMPLE}}^{-1}\mathcal{A}$*. The grid with* 80×40 *cells is used.*

BFS case. The planned future research includes the improvement of allowing robustness with respect to mesh refinement on turbulent calculations.

5.5. Numerical experiments on the laminar FP case. The modified AL preconditioner is often utilized due to the reduced complexity of solving the subsystem with $\widetilde{Q}_\gamma$, compared to Q_γ involved in the ideal AL preconditioner. The extreme eigenvalues of $\mathcal{P}_{\mathrm{MAL}}^{-1}\mathcal{A}_\gamma$ with the new Schur approximation $\widetilde{S}_{\gamma\ \mathrm{new}}$ are shown in Figure 12. There are two observations to be made. First, for moderate values of γ, e.g., $\gamma \in [0.01,\ 0.1]$, the smallest eigenvalues are far from zero. Second, $\gamma = 0.1$ results in the smallest ratio between the largest and smallest magnitudes of the eigenvalues. Thus, we expect that the optimal value of γ is $\gamma_{\mathrm{opt}} = 0.1$ for the laminar FP case. The prediction is confirmed by Figure 13, which illustrates that $\gamma_{\mathrm{opt}} = 0.1$ results in the fastest convergence rate among other tested values of γ.

In [32] we find out that for the laminar FP case the optimal value of γ for the old Schur approximation $\widetilde{S}_{\gamma\ \mathrm{old}}$ is $\gamma_{\mathrm{opt}} = 400$. Seen from Table 3, on the laminar FP case the modified AL preconditioner with the new Schur approximation $\widetilde{S}_{\gamma\ \mathrm{new}}$ and $\gamma_{\mathrm{opt}} = 0.1$ reduces the number of the Krylov subspace iterations by factors 14.6

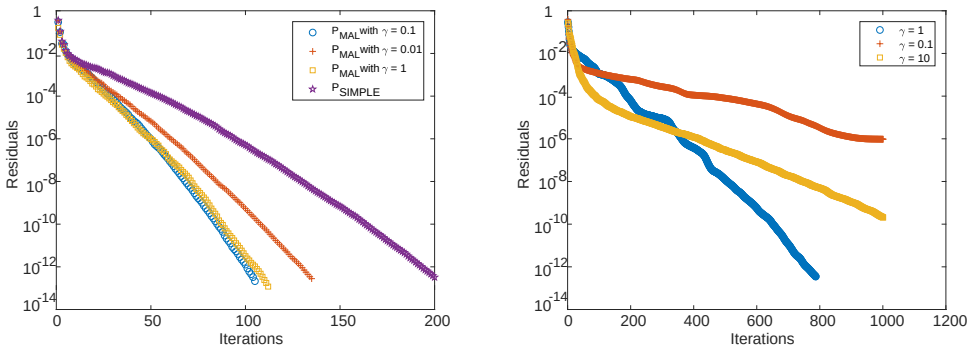

(a) $\mathcal{P}_{\text{MAL}}$ with $\widetilde{S}_{\gamma\ \text{new}}$ and $\mathcal{P}_{\text{SIMPLE}}$ (b) $\mathcal{P}_{\text{MAL}}$ with $\widetilde{S}_{\gamma\ \text{old}}$

FIG. 11. *Turbulent BFS: the convergence of GMRES (no restart) preconditioned by the modified AL preconditioner* $\mathcal{P}_{\text{MAL}}$ *with the new Schur approximation* $\widetilde{S}_{\gamma\ \text{new}}$ *and the SIMPLE preconditioner (left), and the modified AL preconditioner* $\mathcal{P}_{\text{MAL}}$ *with the old Schur approximation* $\widetilde{S}_{\gamma\ \text{old}}$ *(right). The grid with* 9600 *cells is used.*

TABLE 2

Turbulent BFS: the number of GMRES iterations (no restart) preconditioned by the AL preconditioners with different Schur complement approximations and different values of γ*, and the SIMPLE preconditioner. The grid with* 9600 *cells is used.*

γ	0.01	0.1	1
$\mathcal{P}_{\text{IAL}}$ with $\widetilde{S}_{\gamma\ \text{new}}$:	133	103	96
$\mathcal{P}_{\text{MAL}}$ with $\widetilde{S}_{\gamma\ \text{new}}$:	134	104	111
$\mathcal{P}_{\text{MAL}}$ with $\widetilde{S}_{\gamma\ \text{old}}$:	> 1000	> 1000	791
$\mathcal{P}_{\text{SIMPLE}}$:	199		

and 2.2, compared to the old Schur approximation $\widetilde{S}_{\gamma\ \text{old}}$ with $\gamma_{\text{opt}} = 400$ and the SIMPLE preconditioner, respectively. The above numerical results clearly show that the new Schur complement approximation $\widetilde{S}_{\gamma\ \text{new}}$ proposed in this paper significantly improves the performance of the AL preconditioner for laminar flows too.

In the previous work [32] we set the stopping tolerance for the linear system to be 10^{-3} in the laminar FP case and compare the modified AL preconditioner with the old Schur complement approximation and the SIMPLE preconditioner in terms of the number of Krylov subspace iterations. This comparison is executed based on the chosen stopping tolerance which balances the linear and nonlinear solvers. Since the nonlinear solver is not the focus of this paper, it is reasonable to solve the linear system to the machine accuracy so that a comprehensive evaluation of the proposed new Schur complement approximation in the AL preconditioner and a complete comparison with the old Schur complement approximation and the SIMPLE preconditioner can be obtained. In this sense, the results in Table 3, regarding the number of Krylov subspace iterations preconditioned by the modified AL preconditioner with the old Schur complement approximation and the SIMPLE preconditioner, supplement the previous work [32].

5.6. Comparisons between the turbulent and laminar calculations. Finally we put the turbulent and laminar results together in Table 4 for a comparison. Considering the modified AL preconditioner with the new Schur approximation $\widetilde{S}_{\gamma\ \text{new}}$ and the optimal value γ_{opt} , we see that the number of the Krylov subspace iterations

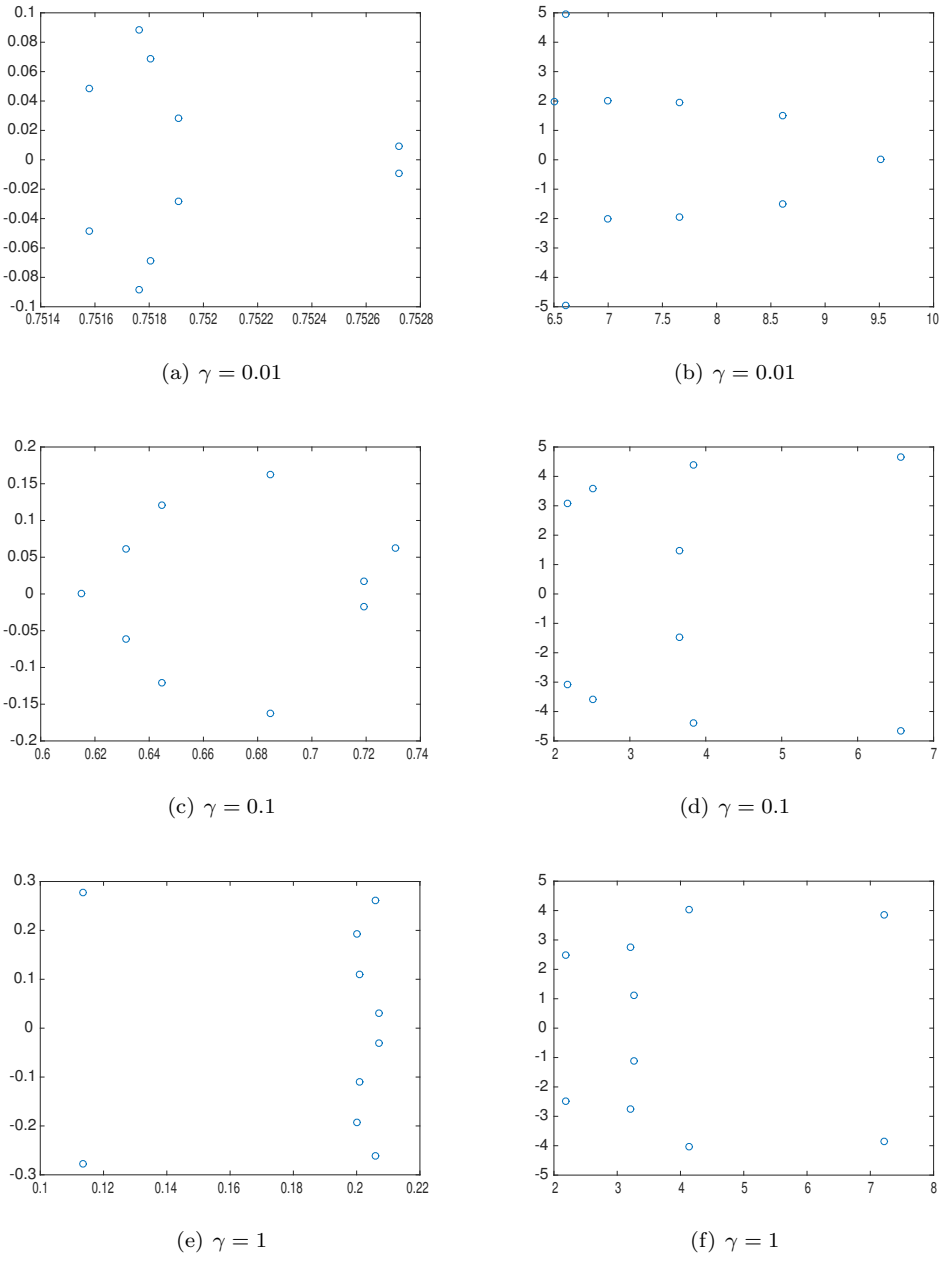

(a) $\gamma = 0.01$ (b) $\gamma = 0.01$

(c) $\gamma = 0.1$ (d) $\gamma = 0.1$

(e) $\gamma = 1$ (f) $\gamma = 1$

FIG. 12. *Laminar FP: the ten smallest (left) and largest (right) eigenvalues of* $\mathcal{P}_{\mathrm{MAL}}^{-1}\mathcal{A}_\gamma$ *with the new Schur approximation* $\widetilde{S}_{\gamma\ \mathrm{new}}$ *and different values of* γ. *The grid with* 64×64 *cells is used.*

is quite acceptable for all tested cases. This means that the new Schur complement approximation proposed in this paper makes the AL preconditioner robust with respect to the mesh anisotropy and physical parameter variation, e.g., the variation of the viscosity. Regarding the optimal value of γ, it lies in the interval $[0.1,\ 1]$ for all

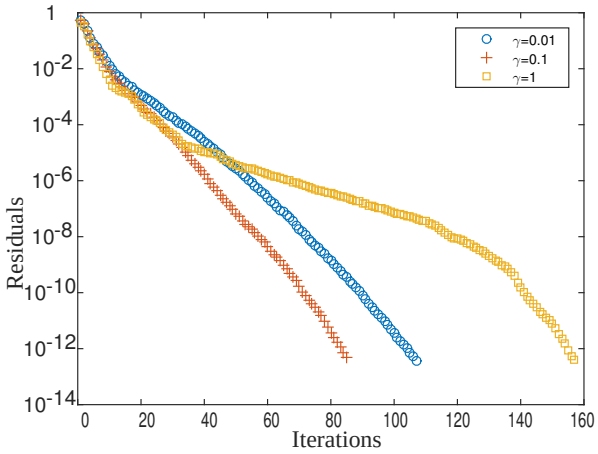

FIG. 13. *Laminar FP: the convergence of GMRES (no restart) preconditioned by the modified AL preconditioner with the new Schur complement approximation* $\widetilde{S}_{\gamma\ \mathrm{new}}$ *and different values of* γ. *The grid with* 64×64 *cells is used.*

TABLE 3

Laminar FP: the number of GMRES iterations (no restart) preconditioned by the modified AL preconditioner with two Schur complement approximations and their corresponding optimal values of γ, *and the SIMPLE preconditioner. The grid with* 64×64 *cells is used.*

$\mathcal{P}_{\mathrm{MAL}}$ with $\widetilde{S}_{\gamma\ \mathrm{new}}$ and $\gamma_{\mathrm{opt}} = 0.1$	$\mathcal{P}_{\mathrm{MAL}}$ with $\widetilde{S}_{\gamma\ \mathrm{old}}$ and $\gamma_{\mathrm{opt}} = 400$	$\mathcal{P}_{\mathrm{SIMPLE}}$
83	1200	183

tests when applying the new Schur complement approximation in the modified AL preconditioner. This interval is much more clustered than when using the old Schur complement approximation. This means that the optimal value γ_{opt} is easier to determine and weakly problem dependent for the new variant. Regarding the influence of γ on the convergence, we observe that by using the new Schur complement approximation the variation of the convergence rate arising from different values of γ is much less than that with the old approximation. See Figure 11 for the turbulent BFS case, for instance. This illustrates that the new AL variant is less sensitive to the values of γ. In addition, the advantage of the new Schur approximation over the old one is clearly exhibited in terms of the significantly reduced number of Krylov subspace iterations in all cases. This means that the new Schur approximation can considerably improve the efficiency of the AL preconditioner for both turbulent and laminar calculations. Although the number of Krylov subspace iterations by applying the modified AL preconditioner with new Schur approximation and the optimal value of γ is less than the SIMPLE preconditioner, the benefit in terms of the total wall-clock time needs the further assessment due to the heavier cost of the AL preconditioner presented in section 4. This is included in the future research plan.

6. Conclusion and future work. In this paper, we have considered the extension of the AL preconditioner in the context of stabilized finite volume methods to both laminar flow governed by the Navier–Stokes equations and turbulent flow governed by the Reynolds-averaged Navier–Stokes (RANS) equations with eddy-viscosity turbulence model.

TABLE 4

The number of GMRES iterations (no restart) accelerated by different preconditioners on different tests. The grids with 80×40 *cells,* 9600 *cells, and* 64×64 *cells are used for the turbulent FP, turbulent BFS, and laminar FP cases, respectively.*

	Turbulent FP	Turbulent BFS	Laminar FP
$\mathcal{P}_{\text{MAL}}$ with $\widetilde{S}_{\gamma\ \text{new}}$			
γ_{opt}:	1	0.1	0.1
iterations:	140	104	83
$\mathcal{P}_{\text{MAL}}$ with $\widetilde{S}_{\gamma\ \text{old}}$			
γ_{opt}:	1	1	400
iterations:	> 5000	791	1200
$\mathcal{P}_{\text{SIMPLE}}$			
iterations:	180	199	183

We find out that a straightforward application of the AL preconditioner to the RANS equations yields disappointing results and therefore proposed a new Schur complement approximation which leads to a variant of the AL preconditioner. The approach is to substitute the approximation of the Schur complement from the SIMPLE preconditioner into the inverse of the Schur complement for the AL preconditioner. Without the contradictory requirements in the old approximation, the new Schur complement approximation makes the new AL variant less sensitive to the choice of γ and weakly problem dependent.

To evaluate the new variant of the AL preconditioner, we consider the solution of the linear system obtained at the 30th nonlinear iteration for three cases: laminar and turbulent boundary-layer flow over a flat plate on grids with large aspect ratios, and turbulent flow over a backward-facing step in a channel. The backward-facing step flow is more complicated than the flat-plate flow as it features separation, a free shear-layer, and reattachment. The new variant of the AL preconditioner significantly speeds up the convergence rate of the Krylov subspace solvers for both turbulent and laminar cases. Spectral analysis of the preconditioned systems explains the observed difference. Like the SIMPLE preconditioner, the new AL variant avoids the clustering of the smallest eigenvalues near zero. At the same time, the largest eigenvalues by applying the new AL variant are significantly smaller than the SIMPLE preconditioner. As a consequence, the new variant of the AL preconditioner outperforms the considered preconditioners in terms of the number of Krylov subspace iterations. The matrices and right-hand side vectors used in this paper are publicly available on the website [18]. This makes the research reproducible and the comparison with other preconditioning techniques easier.

We present a basic cost model to compare the new variant with others, including the SIMPLE preconditioner, which is well established for the RANS equations. The heavier cost of the new AL variant can be paid off with fewer Krylov subspace iterations, which is seen in this paper. However, our test cases so far have been carried out on the modest grid sizes that allow the matrices to be exported and analyzed in MATLAB. Future work is planned on the assessment of the new AL variant on larger grid sizes to show the benefit in terms of the reduced total wall-clock time. In this paper we observe that the new AL variant is not mesh independent. Another planned future research is on the improvement which allows robustness with respect to mesh refinement.

REFERENCES

[1] M. Benzi, G. Golub, and J. Liesen, *Numerical solution of saddle point problems*, Acta Numer., 14 (2005), pp. 1–137.

[2] M. Benzi and M. A. Olshanskii, *An augmented Lagrangian-based approach to the Oseen problem*, SIAM J. Sci. Comput., 28 (2006), pp. 2095–2113, https://doi.org/10.1137/050646421.

[3] M. Benzi, M. Olshanskii, and Z. Wang, *Modified augmented Lagrangian preconditioners for the incompressible Navier-Stokes equations*, Internat. J. Numer. Methods Fluids, 66 (2011), pp. 486–508.

[4] M. Benzi and Z. Wang, *Analysis of augmented Lagrangian-based preconditioners for the steady incompressible Navier–Stokes equations*, SIAM J. Sci. Comput., 33 (2011), pp. 2761–2784, https://doi.org/10.1137/100797989.

[5] M. Benzi and Z. Wang, *A parallel implementation of the modified augmented Lagrangian preconditioner for the incompressible Navier-Stokes equations*, Numer. Algorithms, 64 (2013), pp. 73–84.

[6] D. Driver and H. Seegmiller, *Features of a reattaching turbulent shear layer in divergent channel flow*, AIAA J., 23 (1985), pp. 163–171.

[7] L. Eça, G. Vaz, and M. Hoekstra, *A verification and validation exercise for the flow over a backward facing step*, in Proceedings of the Fifth European Conference on Computational Fluid Dynamics ECCOMAS CFD 2010, J. Pereira and A. Sequeria, eds., Lisbon, Portugal, 2010.

[8] H. Elman, V. E. Howle, J. Shadid, R. Shuttleworth, and R. Tuminaro, *Block preconditioners based on approximate commutators*, SIAM J. Sci. Comput., 27 (2006), pp. 1651–1668, https://doi.org/10.1137/040608817.

[9] H. Elman, D. Silvester, and A. Wathen, *Finite Elements and Fast Iterative Solvers: With Applications in Incompressible Fluid Dynamics*, Oxford University Press, 2014.

[10] ERCOFTAC, *Classic Collection Database*, http://www.ercoftac.org/products_and_services/classic_collection_database/.

[11] J. Ferziger and M. Peric, *Computational Methods for Fluid Dynamics*, Springer Science & Business Media, 2012.

[12] X. He, M. Neytcheva, and C. Vuik, *On an augmented Lagrangian-based preconditioning of Oseen type problems*, BIT, 51 (2011), pp. 865–888.

[13] D. Kay, D. Loghin, and A. Wathen, *A preconditioner for the steady-state Navier–Stokes equations*, SIAM J. Sci. Comput., 24 (2002), pp. 237–256, https://doi.org/10.1137/S106482759935808X.

[14] C. Klaij, *On the stabilization of finite volume methods with co-located variables for incompressible flow*, J. Comput. Phys., 297 (2015), pp. 84–89.

[15] C. Klaij, X. He, and C. Vuik, *On the design of block preconditioners for maritime engineering*, in Proceedings of the Seventh International Conference on Computational Methods in Marine Engineering MARINE, M. Visonneau, P. Queutey, and D. L. Touzé, eds., Nantes, France, 2017.

[16] C. Klaij and C. Vuik, *SIMPLE-type preconditioners for cell-centered, colocated finite volume discretization of incompressible Reynolds-averaged Navier-Stokes equations*, Internat. J. Numer. Methods Fluids, 71 (2013), pp. 830–349.

[17] C. Li and C. Vuik, *Eigenvalue analysis of the SIMPLE preconditioning for incompressible flow*, Numer. Linear Algebra Appl., 11 (2004), pp. 511–523.

[18] Maritime Research Institute Netherlands, *ReFRESCO Linear Systems*, http://www.refresco.org/publications/data-sharing/linear-systems/.

[19] Maritime Research Institute Netherlands, *ReFRESCO Web page*, http://www.refresco.org.

[20] F. Menter, *Two-equation eddy-viscosity turbulence models for engineering applications*, AIAA J., 32 (1994), pp. 1598–1605.

[21] T. Miller and F. Schmidt, *Use of a pressure-weighted interpolation method for the solution of the incompressible Navier-Stokes equations on a nonstaggered grid system*, Numer. Heat Transfer A Appl., 14 (1988), pp. 213–233.

[22] M. A. Olshanskii and E. E. Tyrtyshnikov, *Iterative Methods for Linear Systems: Theory and Applications*, SIAM, 2014, https://doi.org/10.1137/1.9781611973464.

[23] P. Patankar, *Numerical Heat Transfer and Fluid Flow*, McGraw-Hill, New York, 1980.

[24] J. Pestana and A. J. Wathen, *Natural preconditioning and iterative methods for saddle point systems*, SIAM Rev., 57 (2015), pp. 71–91, https://doi.org/10.1137/130934921.

[25] D. Rijpkema, *Flat Plate in Turbulent Flow*, Tech. Report 23279-1-RD, Maritime Research Institute Netherlands, 2009.

[26] Y. Saad, V. der Vorst, and A. Henk, *Iterative solution of linear systems in the* 20*th century*, J. Comput. Appl. Math., 123 (2000), pp. 1–33.
[27] A. Segal, M. ur Rehman, and C. Vuik, *Preconditioners for incompressible Navier-Stokes solvers*, Numer. Math. Theory Methods Appl., 3 (2010), pp. 245–275.
[28] D. Silvester, H. Elman, D. Kay, and A. Wathen, *Efficient preconditioning of the linearized Navier-Stokes equations for incompressible flow*, J. Comput. Appl. Math., 128 (2001), pp. 261–279.
[29] C. Vuik, A. Saghir, and G. Boerstoel, *The Krylov accelerated SIMPLE(R) method for flow problems in industrial furnaces*, Internat. J. Numer. Methods Fluids, 33 (2000), pp. 1027–1040.
[30] P. Wesseling, *Principles of Computational Fluid Dynamics*, Springer Science & Business Media, 2009.
[31] F. White, *Fluid Mechanics*, McGraw-Hill, 1994.
[32] X.He, C. Vuik, and C.M. Klaij, *Block-preconditioners for the incompressible Navier-Stokes equations discretized by a finite volume method*, J. Numer. Math., 25 (2017), pp. 89–105.